Impact of increased hematocrit on right ventricular afterload in response to chronic hypoxia

David A. Schreier, Timothy A. Hacker, Kendall Hunter, Jens Eickoff, Aiping Liu, Gouqing Song and Naomi Chesler

J Appl Physiol 117:833-839, 2014. First published 28 August 2014; doi:10.1152/japplphysiol.00059.2014

J Appl Physiol 117: 833–839, 2014.
First published August 28, 2014; doi:10.1152/japplphysiol.00059.2014.

Impact of increased hematocrit on right ventricular afterload in response to chronic hypoxia

David A. Schreier,[1] Timothy A. Hacker,[2] Kendall Hunter,[3] Jens Eickoff,[2] Aiping Liu,[1] Gouqing Song,[2] and Naomi Chesler[1,2]

[1]*Department of Biomedical Engineering University of Wisconsin, Madison, Wisconson;* [2]*Department of Medicine Medical Science Center, Madison, Wisconsin; and* [3]*Department of Bioengineering University of Colorado, Aurora, Colorado*

Submitted 27 January 2014; accepted in final form 20 August 2014

Schreier DA, Hacker TA, Hunter K, Eickoff J, Liu A, Song G, Chesler N. Impact of increased hematocrit on right ventricular afterload in response to chronic hypoxia. *J Appl Physiol* 117: 833–839, 2014. First published August 28, 2014; doi:10.1152/japplphysiol.00059.2014.—Chronic hypoxia causes chronic mountain sickness through hypoxia-induced pulmonary hypertension (HPH) and increased hematocrit. Here, we investigated the impact of increased hematocrit and HPH on right ventricular (RV) afterload via pulmonary vascular impedance. Mice were exposed to chronic normobaric hypoxia (10% oxygen) for 10 (10H) or 21 days (21H). After baseline hemodynamic measurements, ~500 μl of blood were extracted and replaced with an equal volume of hydroxyethylstarch to normalize hematocrit and all hemodynamic measurements were repeated. In addition, ~500 μl of blood were extracted and replaced in control mice with an equal volume of 90% hematocrit blood. Chronic hypoxia increased input resistance (Z_0 increased 82% in 10H and 138% in 21H vs. CTL; $P < 0.05$) and characteristic impedance (Z_C increased 76% in 10H and 109% in 21H vs. CTL; $P < 0.05$). Hematocrit normalization did not decrease mean pulmonary artery pressure but did increase cardiac output such that both Z_0 and Z_C decreased toward control levels. Increased hematocrit in control mice did not increase pressure but did decrease cardiac output such that Z_0 increased. The paradoxical decrease in Z_C with an acute drop in hematocrit and no change in pressure are likely due to inertial effects secondary to the increase in cardiac output. A novel finding of this study is that an increase in hematocrit affects the pulsatile RV afterload in addition to the steady RV afterload (Z_0). Furthermore, our results highlight that the conventional interpretation of Z_C as a measure of proximal artery stiffness is not valid in all physiological and pathological states.

cardiopulmonary hemodynamics; chronic hypoxia; characteristic impedance; blood viscosity; pulmonary vascular impedance

CHRONIC MOUNTAIN SICKNESS (CMS), also known as Monge's disease, occurs after chronic exposure to hypoxia at high altitudes and is characterized by increased pulmonary artery pressures and pulmonary vascular resistance (29) as well as increased hematocrit (19). Chronic hypoxia also contributes to worse outcomes in lung diseases such as chronic obstructive pulmonary disease, sleep apnea, and pulmonary fibrosis (1, 10, 15). In preclinical animal models of pulmonary arterial hypertension (PAH), chronic hypoxia is often used to generate hypoxia-induced pulmonary hypertension (HPH). PAH is a debilitating disease with a low median survival of 2.8 yr (6, 17) and is characterized by remodeling throughout the pulmonary vasculature, including distal arterial narrowing and proximal and distal pulmonary artery stiffening, leading to right ventricular (RV) dysfunction that progresses to RV failure as the cause of death (28). HPH in rodents recapitulates the pulmonary vascular remodeling and RV hypertrophy that occur in patients with PAH but also increases hematocrit. Indeed, the increase in hematocrit can be dramatic, from ~40 to ~70% in only a few days (12).

Increased hematocrit increases blood viscosity (2, 4, 32, 47), which has been shown to substantially increase both systemic and pulmonary vascular resistance (2, 5, 13, 16, 47). Independent of the increase in blood viscosity, hypoxia increases resistance acutely via hypoxic pulmonary vasoconstriction and chronically via pulmonary vascular remodeling (2, 27, 33, 40). The independent effects of these blood and vessel wall changes on RV afterload have received minimal attention traditionally (16). Investigation into changes in RV afterload, as a result of the increase in hematocrit, in response to chronic hypoxia could potentially lend valuable insight into the role of increased hematocrit in CMS and other lung diseases.

The most comprehensive measure of RV afterload is pulmonary vascular impedance (PVZ). Whereas resistance represents the opposition to steady flow in a vascular bed, which is largely generated by friction in small diameter vessels, impedance represents the opposition to pulsatile flow, which can be generated by stiff vessels that do not accommodate pulsations, branching, and tapering vessels that generate wave reflections, and other phenomena. The impedance to steady flow, i.e., the resistance, is represented by Z_0; the impedance to high frequency pulsations generated by narrow, stiff vessels, i.e., the characteristic impedance, is represented by Z_C; and the degree of pulse wave reflections is represented by the index of wave reflection P_b/P_f. In PAH, pulmonary arterial stiffness, which is related to Z_C, is an excellent predictor of mortality from RV failure (11, 14, 18, 22, 26).

Here, we sought to investigate the impact of hematocrit on RV afterload by quantifying changes in PVZ in response to chronic hypoxia. We hypothesize that increasing hematocrit due to chronic hypoxia would be a significant contributor to Z_0 and a mild or nonexistent contributor to Z_C. To test this hypothesis, we measured PVZ in live mice in situ with and without exposure to chronic hypoxia. Then, we normalized hematocrit to control levels in hypoxic mice and again measured pulmonary vascular impedance. Our results demonstrate that hematocrit is an important contributor to increased RV afterload in chronic hypoxia. To the best of our knowledge, we are the first to quantify how increased hematocrit contributes to RV afterload independent of pulmonary vascular remodeling.

Address for reprint requests and other correspondence: N. Chesler, 2146 Engineering Centers Bldg., 1550 Engineering Dr., Madison, WI 53706 (e-mail: chesler@engr.wisc.edu).

METHODS

Materials. Male C57BL6/J mice, 12–13 wk old, were obtained from Jackson Laboratory (Bar Harbor, ME) and exposed to room air (CTL, $n = 13$) or chronic normobaric hypoxia (10% oxygen) for either 10 (10H, $n = 7$) or 21 (21H, $n = 7$) days. Normobaric hypoxia was created in environmentally controlled chambers in which nitrogen was mixed with room air; oxygen levels were measured with a sensor in the chamber (Servoflo, Lexington, MA) that controlled a relay valve on the nitrogen gas inflow line via a custom-built closed loop control system. The chamber was opened for 10–20 min three times per week to clean cages and replenish food and water. All mice were exposed to a 12-h light-dark cycle. The University of Wisconsin Institutional Animal Care and Use Committee approved all procedures.

In vivo hemodynamic measurements. Mice were anesthetized with an intraperitoneal injection of urethane solution (2 mg/g body wt), intubated, and placed on a ventilator (Harvard Apparatus, Holliston, MA) using a tidal volume of ~225 μl and respiratory rate of ~200 breaths/min of room air. Mice were then placed supine on a heated pad to maintain body temperature at 38–39°C. A central midline skin incision was made from the lower mandible inferior to the xiphoid process. The thoracic cavity was entered through the sternum, and the chest was carefully removed to expose the right ventricle. To confirm the absence of systemic hypertension, the right carotid artery was cannulated with a 1.2-F catheter-tip pressure transducer (Scisense, London, ON, Canada) and advanced into the ascending aorta. Hydroxyethylstarch was used to restore vascular volume due to blood loss as done previously (33). Subsequently, the apex of the right ventricle was localized and a 1.0-F pressure-tip catheter (Millar Instruments, Houston, TX) was introduced using a 20-gauge needle leaving the pericardium otherwise intact. After instrumentation was established and pressure was stabilized, the catheter was advanced to the main pulmonary artery for measurement. Pressure tracings were recorded at 5 kHz on a hemodynamic workstation (Cardiovascular Engineering, Norwood, MA). Flow measurement was performed via ultrasound (Visualsonics, Toronto, ON, Canada) with a 40-MHz probe during catheterization and recorded with the same system.

Flow was calculated by velocity time integral using spectral analysis of the digitized broadband Doppler audio signal obtained in the main pulmonary artery just distal to the pulmonary valve with the probe in a right parasternal long-axis orientation in the same location as the catheter. The probe was angled until the maximal velocity signal was obtained. Measurement at this point allows for better detection of the main pulmonary arterial inner diameter (MPA ID). Measurement of the MPA ID was taken using the long axis view from leading edge to leading edge during end systole from three different cardiac cycles; we report the average of those three.

We used MPA ID to convert the instantaneous flow velocity signal to instantaneous volume flow rate (Q) assuming a circular cross section and a blunt velocity profile. The signals were visually checked for quality and recorded for later analysis.

After all measurements were completed in the 10H and 21H groups, ~500 μl of blood were extracted and replaced with an equal volume of hydroxyethylstarch to normalize hematocrit to CTL levels based on pilot studies. After a 5-min stabilizing period, all hemodynamic measurements were repeated in this normalized-hematocrit state for mice exposed to chronic hypoxia for 10 days (10H-N_{Hct}) and 21 days (21H-N_{Hct}). Before euthanasia, a 500-μl sample of the normalized-hematocrit blood was taken for analysis. Measurements performed on the extracted blood samples included viscosity using a cone and plate viscometer, blood gas and ion concentrations using an I-STAT portable analyzer and CG8+ cartridge, and hematocrit using a centrifuge.

After all measurements were completed in a group of CTL mice, ~500 μl of blood were extracted and replaced with an equal volume of a 90% hematocrit suspension. To create the 90% hematocrit suspension, whole blood was removed from the left ventricle of C57Bl6 donor mice and then transferred to 50-ml conical tube and centrifuged at 500 *g* for 15 min at room temperature, and blood plasma was removed. The red blood cell pellet was then resuspended at 10 times red blood cell pellet volume in osmolality balanced saline solution and centrifuged again at 500 *g* for 15 min. This process was repeated four times. Finally, washed red blood cells were resuspended to a target hematocrit of 90%. Five minutes after this high hematocrit blood was administered to CTL mice, all hemodynamic measurements were repeated (CTL-H1) and then, blood extraction and replacement and all measurements were repeated a second time (CTL-H2).

In vivo hemodynamic calculations. The instantaneous volume flow and the pressure waveforms were signal-averaged using the ECG as a fiducial point and then processed and analyzed using custom software (Cardiovascular Engineering, Norwood, MA). Twenty consecutive cardiac cycles free of extrasystolic beats were selected and averaged. PVZ was calculated using wave intensity analysis as previously described (25, 34). Total pulmonary vascular resistance (Z_0) was calculated as mean pulmonary arterial pressure (mPAP) divided by Q averaged over the cardiac cycle (i.e., CO). Total pulmonary arterial compliance was calculated from an exponential fit to the pulmonary arterial pressure decay during diastole (31). Characteristic impedance (Z_C) was calculated from the ratio of the change in pressure to the change in flow in early ejection. That is, $Z_C = \frac{dP}{dQ}$, where dP and dQ are taken before when Q reaches 95% of its maximum value. An assumption inherent in this calculation is that the system is free from reflections because the reflected waves do not have time to return to the proximal bed so early in the cardiac cycle (25). To allow further comparison of our data to the existing literature, we calculated pulse wave velocity (PWV) as $PWV = \frac{Z_c * A}{\rho}$ assuming the density of blood $\rho = 1{,}060$ kg/m^3 and cross-sectional area $A = \pi/4$ (MPA ID)^2. Finally, also based on Z_C, the pulmonary arterial pressure waveform was separated into forward (P_f) and backward (P_b) traveling components using the linear wave separation method (42). The index of global wave reflections was calculated as the ratio of the amplitude of P_b to P_f.

Statistical analysis. A limitation of the long axis view for calculating MPA ID is the screen resolution of the ultrasound system (80 μm). Therefore, we performed a bootstrap analysis as a nonparametric technique to determine the effects of screen limitation on our calculation of Z_C. The application of bootstrap yields a number N of resamples of each of our original calculated Z_C values per mouse to determine the true error per measurement associated with our technique (8).

For each group, the significances of the overall changes in parameters with exposure to chronic normobaric hypoxia were assessed using a one-way ANOVA for condition or generalized least squares for repeated measurements with normalized hematocrit. When the ANOVA reached statistical significance, Tukey's multiple comparisons were used for post hoc analysis. Data were considered significant for P values <0.05. All data are presented in terms of means ± standard error. Statistical analysis was performed using R software (Foundation for Statistical Computing, version 2.14.0).

RESULTS

Morphometric effects of chronic hypoxia. The average body weight of the CTL mice was higher than the 10H and 21H groups (Table 1). The left ventricular weight normalized by body weight did not change between groups (Table 1). RV hypertrophy measured both by RV mass normalized by body weight and Fulton index (RV/LV + S) increased with 10 days of hypoxia and continued to increase with 21 days of hypoxia (Table 1).

Table 1. *Body weight, ventricular weights, and Fulton index for combined CTL, 10H, and 21H mice*

	CTL	10H	21H
BW, g	26.4 ± 0.7	23.0 ± 0.3*	22.5 ± 0.5*
RV/BW, mg/g	0.90 ± 0.02	1.06 ± 0.05*	1.31 ± 0.03*†
LV +S/BW, mg/g	3.3 ± 0.1	3.1 ± 0.1	3.3 ± 0.2
Fulton index, RV/LV +S	0.28 ± 0.01	0.34 ± 0.01*	0.40 ± 0.01*†

Values are means ± SE; $n = 13$ for control (CTL), $n = 7$ for chronic normobaric hypoxia for 10 days (10H), and $n = 7$ for chronic normobaric hypoxia for 21 days (21H). BW, body weight; RV, right ventricular; LV, left ventricular; S, septum. *$P < 0.05$ vs. CTL; †$P < 0.05$ vs. 10H.

Hemodynamic effects of chronic hypoxia. As expected, hematocrit increased with 10 days of chronic hypoxia and remained elevated with 21 days (Table 2). Similarly, mPAP increased with 10 days of chronic hypoxia and remained elevated with 21 days (Table 2). Cardiac output and stroke volume tended to decrease with increasing duration of hypoxia and were significantly decreased by 21 days (Table 2; $P < 0.05$ for 21H vs. CTL). Pulmonary vascular resistance Z_0 increased after 10 days of hypoxia and was further increased after 21 days of hypoxia (Fig. 1). Characteristic impedance (Z_C) (Fig. 2), systolic pulmonary artery pressure (sPAP), and PWV increased with 10 days of chronic hypoxia and remained elevated with 21 days. Pulmonary arterial compliance decreased with 10 days of chronic hypoxia and remained decreased with 21 days (Fig. 3). Heart rate did not change with chronic hypoxia.

Hemodynamic effects of hematocrit. An exchange of ~500 μl of blood with hydroxyethylstarch decreased hematocrit by 39 to ~43% for 10H-N_{Hct} and 21H-N_{Hct} mice, which was similar to the control mice (Table 2). The change in hematocrit had no effect on the mPAP, sPAP, or pulse pressure but increased cardiac output and stroke volume (significant at 10 days only) (Table 2); heart rate was also decreased in the 10H-N_{Hct} group. Consequently, Z_0 was lower in the 10H-N_{Hct} and 21H-N_{Hct} groups compared with the 10H and 21H groups, respectively (Fig. 1). Z_C was lower in the 10H-N_{Hct} and 21H-N_{Hct} groups compared with the 10H and 21H groups, respectively, and was similar to the CTL group value (Fig. 2).

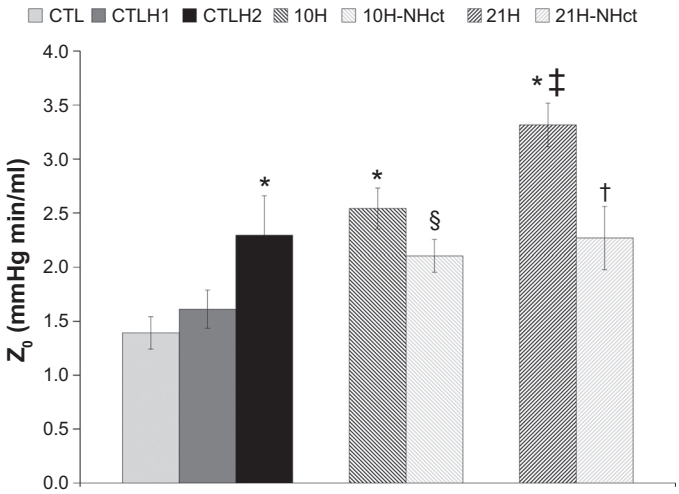

Fig. 1. Input resistance Z_0 calculated as mean pulmonary arterial pressure/CO. CTL-H1 and CTL-H2, first and second hemodynamic measurements. *$P <$ 0.05 vs. control (CTL); §$P < 0.05$, normalized-hematocrit state for mice exposed to chronic hypoxia for 10 days (10H-N_{Hct}) vs. chronic normobaric hypoxia (10% oxygen) for 10 days (10H); ‡$P < 0.05$ vs. 10H; †$P < 0.05$ 21H-N_{Hct} vs. 21H.

Pulmonary arterial compliance increased in the 10H-N_{Hct} and 21H-N_{Hct} groups compared with the 10H and 21H groups, respectively, but the change was only significant at 21 days (Fig. 3).

One exchange of ~500 μl of CTL mouse blood with 90% hematocrit suspension increased hematocrit by 38 to ~58%; the second exchange of ~500 μl increased hematocrit overall by 66 to ~70% (Table 3). The increase in hematocrit in CTL mice had no effect on mPAP, sPAP, diastolic (d)PAP, diameter of the main pulmonary arterial, stroke volume, pulse pressure, PWV, or Z_C (Table 3). However, heart rate decreased and therefore cardiac output decreased in the CTL-H1 and CTL-H2 groups. Z_0 tended to increase with the first exchange and became significantly increased after the second exchange with the high hematocrit suspension in CTL mouse lungs (Fig. 1).

The bootstrap analysis of Z_C followed identical trends as the original measurements with increased standard error in each

Table 2. *Hemodynamic parameters derived from pulmonary artery pressure and flow waveforms in combined CTL, 10H, 10H-N_{Hct}, 21H, and 21H-N_{Hct} mice*

	CTL	10H	10H-N_{Hct}	21H	21H-N_{Hct}
Heart rate	562 ± 10	583 ± 4	548 ± 7§	562 ± 14	557 ± 16
Hct, %	42.0 ± 1.2	71.3 ± 1.3*	44.3 ± 1.9§	69.9 ± 1.8*	42.3 ± 2.0†
mPAP, mmHg	15.7 ± 1.6	26.2 ± 1.8*	24.3 ± 1.9	21.3 ± 1.5*	21.3 ± 2.3
dPAP, mmHg	11.0 ± 1.4	20.4 ± 1.6*	18.0 ± 1.6	15.5 ± 1.5	15.7 ± 2.3
sPAP, mmHg	22.4 ± 2.0	37.8 ± 2.5*	37.0 ± 2.5	33.4 ± 1.8*	32.4 ± 2.4
Diameter MPA, mm	1.38 ± 0.02	1.37 ± 0.02	1.39 ± 0.01	1.37 ± 0.01	1.35 ± 0.03
RV cardiac output, ml/min	11.9 ± 0.5	10.7 ± 0.5	12.8 ± 0.5§	9.5 ± 0.5*	10.7 ± 0.5
Stroke volume, μl	21.3 ± 1.0	18.3 ± 0.8	23.3 ± 0.9§	17.1 ± 1.2*	19.3 ± 0.8
Pulse pressure, mmHg	11.4 ± 0.8	17.3 ± 1.6*	19.0 ± 1.0	18.0 ± 0.8*	16.7 ± 0.5
Pulse wave velocity, mm/ms	0.39 ± 0.03	0.67 ± 0.4*	0.49 ± 0.05§	0.81 ± 0.06*	0.42 ± 0.03†
Z_C, mmHg·min^{-1}·ml	0.26 ± 0.02	0.46 ± 0.03*	0.33 ± 0.04§	0.55 ± 0.03*	0.29 ± 0.02†
Z_C (bootstrap method)	0.27 ± 0.07	0.46 ± 0.08*	0.35 ± 0.07	0.56 ± 0.10*	0.28 ± 0.06†
Q_{max}, mm/ms	0.60 ± 0.02	0.55 ± 0.02	0.60 ± 0.01§	0.41 ± 0.01*‡	0.59 ± 0.02†
P_b/P_f	0.28 ± 0.01	0.30 ± 0.03	0.35 ± 0.04	0.32 ± 0.02	0.40 ± 0.03

Values are means ± SE; $n = 13$ for CTL, $n = 7$ for 10H, and 10H-N_{Hct}, and $n = 7$ for 21H and 21H-N_{Hct}. N, normalized; Hct, hematocrit; mPAP, mean pulmonary artery pressure; sPAP, systolic pulmonary artery pressure; dPAP, diastolic pulmonary artery pressure; MPA, main pulmonary artery; RV, right ventricular; Z_C, characteristic impedance; Q_{max}, maximum flow; P_b/P_f, backward and forward pressure waveforms. *$P < 0.05$ vs. CTL; †$P < 0.05$ 21H-N_{Hct} vs. 21H; ‡$P < 0.05$ vs. 10H; §$P < 0.05$ 10H-N_{Hct} vs. 10H.

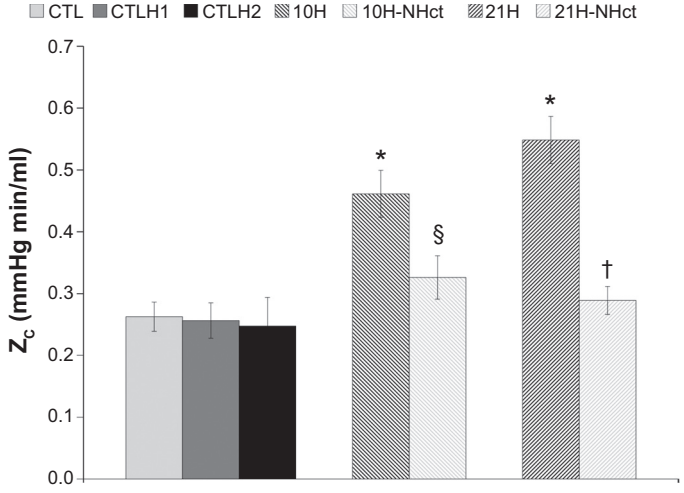

Fig. 2. Characteristic impedance Z_C calculated from pressure/flow (dP/dQ) when Q reaches 95% of its maximal value. *P <0.05 vs. CTL; §P < 0.05 10H-N_{Hct} vs. 10H; †P < 0.05 21H-N_{Hct} vs. 21H.

Table 3. *Hemodynamic parameters derived from pulmonary artery pressure and flow waveforms in separate CTL, CTL-H1, and CTL-H2 mice*

	CTL	CTL-H1	CTL-H2
Heart rate	563 ± 13	522 ± 14*	464 ± 19*
Hct, %	44.7 ± 1.4	58.3 ± 2.0*	69.4 ± 1.6*
mPAP, mmHg	16.4 ± 1.1	15.0 ± 0.9	17.9 ± 2.0
dPAP, mmHg	11.1 ± 1.0	9.7 ± 1.0	12.8 ± 2.3
sPAP, mmHg	22.1 ± 1.3	20.9 ± 1.1	23.4 ± 1.6
Diameter MPA, mm	1.41 ± 0.03	1.41 ± 0.02	1.37 ± 0.03
RV cardiac output, ml/min	12.2 ± 0.8	9.6 ± 0.9*	8.1 ± 0.6*
Stroke volume, μl	21.6 ± 1.4	18.3 ± 1.3	17.3 ± 1.6
Pulse pressure, mmHg	11.1 ± 0.6	11.0 ± 1.0	10.4 ± 1.3
Pulse wave velocity, mm/ms	0.37 ± 0.04	0.40 ± 0.04	0.35 ± 0.05
Z_C, mmHg·min^{-1}·ml	0.24 ± 0.03	0.26 ± 0.03	0.25 ± 0.05
Z_C (Bootstrap method)	0.24 ± 0.09	0.26 ± 0.05	0.26 ± 0.09
Q_{max}, mm/ms	0.62 ± 0.03	0.61 ± 0.04	0.54 ± 0.02
P_b/P_f	0.29 ± 0.02	0.34 ± 0.03	0.40 ± 0.04*

Values are means ± SE; n = 7 for CTL, n = 7 for CTL-H1, and n = 5 for CTL-H2. CTL-H1 and CTL-H2, first and second hemodynamic measurements. *P < 0.05 vs. CTL.

group (Table 2). The increased standard error removed the significant decrease in Z_C between the 10H and 10H-N_{Hct} groups, while the significance between 21H and 21H-N_{Hct} groups was not affected nor was the significance among the CTL, 10H, and 21H groups.

Effects of hematocrit on blood viscosity and blood gases. As expected, blood viscosity increased with chronic hypoxia exposure. The reduction of hematocrit returned blood viscosity to control levels (Table 4). In addition, the transfused (with hydroxyethylstarch) blood in hypoxic animals demonstrated similar shear stress-shear rate curves as the control blood (data not shown). The yield stress was 0.085 ± 0.005 dyn/cm^2 for the CTL group, 0.11 ± 0.01 dyn/cm^2 for both 10H and 21H groups, and 0.074 ± 0.01 dyn/cm^2 for both 10H-N_{Hct} and 21H-N_{Hct} groups in agreement with previous measurements (41). The pH was stable for all five groups: CTL, 10H, 10H-N_{Hct}, 21H, and 21H-N_{Hct} (Table 4). Similarly, the partial pressures for oxygen (pO_2) and carbon dioxide (pCO_2) and blood oxygen saturation (sO_2%) remained constant for all five groups (Table 4). The hemoglobin increased in the 10H and 21H group and the 10H-N_{Hct} and 21H-N_{Hct} groups demonstrated decreased hemoglobin compared with the 10H and 21H groups, respectively (Table 4).

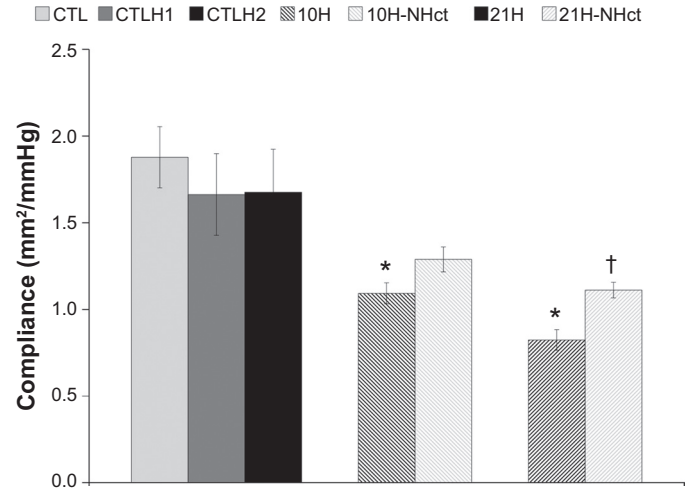

Fig. 3. Total pulmonary arterial compliance from an exponential fit to the pulmonary arterial pressure decay during diastole. *P <0.05 vs. CTL; †P < 0.05 21H-N_{Hct} vs. 21H.

DISCUSSION

The major, novel contribution of this study is the quantification of the impact of the chronic hypoxia-induced increase in hematocrit on the pulsatile components of RV afterload in addition to the steady components of RV afterload (Z_0).

Exchanging ~500 μl of blood with hydroxyethylstarch returned hematocrit and hemoglobin levels in chronic hypoxic mice to near control values (Table 2). For the first time, we quantitatively demonstrate that increases in Z_0, which occur with chronic hypoxia in a mouse model, are decreased with a reduction in hematocrit to control levels. In addition, increasing hematocrit acutely in CTL mice resulted in an increased Z_0 once a hematocrit level of ~70% (CTL-H2, with hematocrit, comparable to that in the 10H and 21H groups) was achieved (Fig. 1). These findings are consistent with a prior study in rats with CMS in which hemodilution from hematocrit of ~70 to ~40% decreased pulmonary vascular resistance (7). Our results are also consistent with a clinical study in which patients with CMS had increased cardiac output and decreased pulmonary artery pressure with hemodilution (44), suggesting decreased resistance with return to a normal hematocrit.

The effect of hematocrit on the unsteady, time-dependent opposition to blood flow is not as simple, since a return to control hematocrit levels decreased Z_C in the mice exposed to 10 and 21 days of hypoxia but an increase in hematocrit to 70% in control mice had no effect on Z_C. Similarly, PWV returns to control levels and pulmonary arterial compliance is improved when hematocrit returns to control levels in chronically hypoxic mice, but there were no changes in PWV or compliance when hematocrit was increased in control mice (Table 2 and Fig. 3). Our results confirm that these metrics do not only reflect arterial wall constitutive behavior but rather are also blood rheology and heart rate dependent.

Table 4. *Arterial blood gas, shear stress and blood viscosity in CTL, 10H, 10H-N_{Hct}, 21H, and 21H-N_{Hct} mice*

	CTL	10H	10H-N_{Hct}	21H	21H-N_{Hct}
pH	7.33 ± 0.04	7.27 ± 0.03	7.24 ± 0.07	7.26 ± 0.03	7.24 ± 0.01
pO_2, mmHg	83.7 ± 9.8	85.7 ± 19.0	81.5 ± 11.2	69.7 ± 6.4	66.0 ± 10.4
sO_2, %	92.0 ± 2.0	93.3 ± 4.2	94.5 ± 1.2	90.7 ± 0.8	89.0 ± 4.9
pCO_2, mmHg	27.8 ± 4.4	29.4 ± 4.7	35.2 ± 7.0	25.4 ± 1.5	23.2 ± 2.6
Hemoglobin, g/dl	14.1 ± 1.0	20.6 ± 0.6*	14.5 ± 0.5§	19.6 ± 0.2*	14.2 ± 0.3†
Shear stress, dyn/cm^2, at $\gamma = 131$ s^{-1}	6.6 ± 0.1	8.1 ± 0.5*	5.7 ± 0.5§	8.4 ± 0.3*	6.1 ± 0.2†
Viscosity, cP at $\gamma = 131$ s^{-1}	5.0 ± 0.1	6.1 ± 0.3*	4.4 ± 0.2§	6.4 ± 0.2*	4.6 ± 0.1†

Values are means ± SE; $n = 6$ for CTL, $n = 7$ for 10H, and $n = 7$ for 21H. pO_2, partial pressure of oxygen; pCO_2, partial pressure of carbon dioxide; sO_2, blood oxygen saturation. *$P < 0.05$ vs. CTL; †$P < 0.05$ 21H-N_{Hct} vs. 21H; §$P < 0.05$ 10H-N_{Hct} vs. 10H.

Characteristic impedance, Z_C, is frequently interpreted as a measure of arterial stiffness. Indeed, in the absence of viscous effects, such as in the artery wall and at the blood-artery interact, Z_C can be approximated as $\sqrt{\frac{\rho * E * h}{2 * \pi^2 * r^5}}$ where E is arterial elastic modulus, h is arterial wall thickness, and r is arterial inner radius (37). However, it is important to note that Z_C can be calculated as the square root of the blood inertance divided by the compliance of the proximal segments of the arterial network (23). When blood inertance is constant, the simplistic relationship between Z_C and compliance (inverse stiffness) is valid. However, when blood inertance is not constant, such as occurs when stroke volume or cardiac output increase due to hematocrit normalization in hypoxic animals (or when cardiac output decreases due to increased hematocrit in control animals) as shown here, these effects must be taken into account.

A more widely applicable definition of Z_C includes Z_L, the longitudinal impedance and Z_T, the transverse impedance as $Z_C = \sqrt{Z_L * Z_T}$. The longitudinal impedance depends on viscosity and Womersley number, which itself depends on radius and the square root of density, heart rate, and inverse of viscosity. Therefore, Z_C increases with the square root of viscosity (24, 43, 45), which is one mechanism by which hematocrit normalization likely decreased Z_C. This suggestion is supported by a prior study by Fischer et al. (9) that demonstrated that blood viscosity has a strong influence on arterial wall elasticity in the systemic circulation. Furthermore, Z_C depends on heart rate, which likely explains the lack of increase in Z_C in the high hematocrit control mice. That is, while increased blood viscosity should increase Z_L and thus Z_C, decreased heart rate should decrease Womersley number and thus Z_L, such that no change in either Z_L or Z_C is a reasonable result.

That said, we cannot exclude an interaction effect between pulmonary vascular remodeling and viscosity that affects pulmonary vascular pulsatile pressure-flow relationships. Experiments conducted in an isolated, ventilated, and perfused lung setup with pulsatile flow (36–38), varying perfusate viscosity, and different states of lung remodeling would be an ideal way to answer this question. Furthermore, in an ex vivo setup, cardiac output, including stroke volume and heart rate, could be kept identical between groups. Finally, since distal arterial stiffness can be measured in an isolated lung experiment (40), if coupled with isolated vessel tests in which proximal arterial stiffness can be directly measured (35), experiments such as these would shed new light on the ways in which Z_C, PWV, and pulse pressure relate to pulmonary arterial stiffness in normal and high hematocrit states.

The reduction of hematocrit to control levels did not affect sPAP, dPAP, mPAP, or pulse pressure in the chronically hypoxic mice (Table 2). Previous clinical studies have demonstrated that small increases in hematocrit tend to decrease mean pulmonary artery pressure, while dramatic increases in hematocrit increase pressure and decrease flow (5, 13). Despite the increased oxygen-carrying capacity of high hematocrit blood, evidence suggests that the increase in vascular resistance decreases peripheral oxygen delivery (21). In addition, our hematocrit normalization reduced the oxygen carrying capacity of the blood. The reduction in oxygen carrying capacity of blood may have been the cause of the significant increase in stroke volume and cardiac output in the 10H-N_{Hct} mice. This suggests that the increases in cardiac output with hematocrit normalization were a regulatory response.

Several limitations should be noted. We did not measure blood density but Wang et al. (39) suggest that blood density changes 1.4% between a hematocrit of ~70 and ~40%. Also, the hydroxyethylstarch added to normalize hematocrit has similar density to plasma (1,077 to 1,060 kg/m^3). The change in yield stress between 10H and 21H mice compared with 10H-N_{Hct} and 21H-N_{Hct} was 33%, and the change in blood viscosity at a shear rate of 131 s^{-1} was 29%. Therefore, we anticipate the effects of potential blood density changes on Z_0 and Z_C would be smaller and less important compared with the effects of viscosity and/or yield stress changes. Also, all hemodynamic measurements were obtained with mice in an anesthetized state, which may affect heart rate and thus cardiac output. However, the normal range of mouse heart rates in a nonanesthetized state is ~460–620 beats/min (30). In our study heart rate only varied from ~522–583 beats/min, with the exception of the 464 beats/min of the CTL-H2 group. This greater consistency of heart rate in the anesthetized state is an advantage since cardiac output will be more consistent between groups. The approach we used to normalize hematocrit in hypoxic mice, blood replacement with a cell-free solution, has been previously used to model hemorrhagic shock, which can lead to microthrombi formation. We used hydroxyethylstarch, which has been shown to limit microthrombi formation (3). Also, we measured hemodynamics ~5 min after hematocrit normalization, which is less than the time in which microthrombi begin to form (~60 min) (20). Repeated hemodilution via replacement of whole blood with hydroxyethylstarch may alter iron reserves in the blood and consequently mean corpuscular volume and pliability of the erythrocytes (46). Given that

hemodilution in this study was acute and only occurred once per animal, red blood cell mechanics should not be altered. Finally, there was insufficient blood volume in each mouse to measure viscosity, arterial blood gases, and mixed venous blood gases. In future work, measuring mixed venous blood gas would provide a validation of the catheter-based CO measurement via the Fick equation.

Our results demonstrate for the first time the effects of increased hematocrit on RV afterload during the progression of hypoxic pulmonary hypertension in mice. The significant changes in Z_C, PWV, and pulmonary arterial compliance in the 10H-N_{Hct} and 21H-N_{Hct} mice suggest that decreasing hematocrit has the beneficial effect of decreasing metrics of pulsatile RV afterload, via increasing blood inertance. Clinically, these results suggest that pulmonary vascular impedance studies within the CMS population could lend valuable insight into possible changes in the pulsatile RV afterload. The return of hematocrit to control levels reduced RV afterload toward control levels, suggesting a possible route to alleviate stress on the RV caused by increased hematocrit in patients with CMS and other forms of HPH.

ACKNOWLEDGMENTS

We thank Dr. Ron R. Magness and Jason Austin for assistance in performing viscosity measurements and analysis.

GRANTS

This study was supported by National Institutes of Health Grants R01-HL-086939 and R01-HL-105598 (to N. Chelser), K25-HL-09749 (to K. Hunter), and HL-49210, HD-38843, and HL-117341 (to R. R. Magness).

DISCLOSURES

No conflicts of interest, financial or otherwise, are declared by the author(s).

AUTHOR CONTRIBUTIONS

Author contributions: D.A.S., T.A.H., G.S., and N.C.C. conception and design of research; D.A.S., T.A.H., and G.S. performed experiments; D.A.S., T.A.H., K.S.H., A.L., and N.C.C. analyzed data; D.A.S., T.A.H., K.S.H., J.E., A.L., and N.C.C. interpreted results of experiments; D.A.S., T.A.H., and N.C.C. prepared figures; D.A.S., T.A.H., and N.C.C. drafted manuscript; D.A.S., T.A.H., K.S.H., J.E., A.L., G.S., and N.C.C. edited and revised manuscript; D.A.S., T.A.H., K.S.H., J.E., A.L., G.S., and N.C.C. approved final version of manuscript.

REFERENCES

1. **Barbera J, Peinado V, Santos S.** Pulmonary hypertension in chronic obstructive pulmonary disease. *Eur Respir J* 21: 892–905, 2003.
2. **Barer G, Bee D, Wach RA, Sheffield S.** Contribution of polycythaemia to pulmonary hypertension in simulated high altitude in rats. *J Physiol* 336: 27–38, 1983.
3. **Cabrales P, Tsai AG, Intaglietta M.** Resuscitation from hemorrhagic shock with hydroxyethyl starch and coagulation changes. *Shock* 28: 461–467, 2007.
4. **Chien S, Usami S, Taylor H, Lundberg J, Gregersen M.** Effects of hematocrit and plasma proteins on human blood rheology at low shear rates. *J Appl Physiol* 21: 81–87, 1966.
5. **Cinar Y, Demir G, Paç M, Cinar A.** Effect of hematocrit on blood pressure via hyperviscosity. *Am J Hypertens* 12: 739–743, 1999.
6. **D'Alonzo G, Barst R.** Survival in patients with primary pulmonary hypertension. Results from a national prospective registry. *Ann Intern Med* 115: 343–349, 1991.
7. **Du HK, Lee YJ, Colice GL, Leiter JC, Ou LC.** Pathophysiological effects of hemodilution in chronic mountain sickness in rats. *J Appl Physiol* 80: 574–582, 1996.
8. **Effron B.** Bootstrap methods: another look at the jackknife. *Ann Stat* 7: 1–26, 1979.
9. **Fischer E, Armentano RL, Pessana FM, Graf S, Romero L, Christen AI, Simon A, Levenson J.** Endothelium-dependent arterial wall tone elasticity modulated by blood viscosity. *Am J Physiol Heart Circ Physiol* 282: H389–H394, 2002.
10. **Fraser KL, Tullis DE, Sasson Z, Hyland RH, Thornley KS, Hanly PJ.** Pulmonary hypertension and cardiac function in adult cystic fibrosis: role of hypoxemia. *Chest* 115: 1321–1328, 1999.
11. **Gan C, Lankhaar J, Westerhof N, Marcus J, Becker A, Twisk J, Boonstra A, Postmus PE, Vonk-Noordegraaf A.** Noninvasively assessed pulmonary artery stiffness predicts mortality in pulmonary arterial hypertension. *Chest* 132: 1906–1912, 2007.
12. **Graber S, Krantz S.** Erythropoietin and the control of red cell production. *Annu Rev Med* 29: 51–66, 1978.
13. **Guilot M, Ross-Ascuitto N, Ascuitto R.** Fluid-flow energetics for curved or angulated pathways associated with staged operations for the modified Fontan procedure. *Congentical Cardiol Today* 10: 1–15, 2012.
14. **Hemnes A, Champion HC.** Right heart function and haemodynamics in pulmonary hypertension. *Int J Clin Pract Suppl* 62: 11–19, 2008.
15. **Hiestand D, Phillips B.** The overlap syndrome: chronic obstructive pulmonary disease and obstructive sleep apnea. *Crit Care Clin* 24: 551–563, 2008.
16. **Hoffman JI.** Pulmonary vascular resistance and viscosity: the forgotten factor. *Pediatr Cardiol* 32: 557–561, 2011.
17. **Humbert M, Sitbon O, Chaouat A, Bertocchi M, Habib G, Gressin V, Yaïci A, Weitzenblum E, Cordier JF, Chabot F, Dromer C, Pison C, Reynaud-Gaubert M, Haloun A, Laurent M, Hachulla E, Cottin V, Degano B, Jaïs X, Montani D, Souza R, Simonneau G.** Survival in patients with idiopathic, familial, and anorexigen-associated pulmonary arterial hypertension in the modern management era. *Circulation* 122: 156–163, 2010.
18. **Hunter KS, Lee P, Lanning CJ, Ivy DD, Kirby KS, Claussen LR, Chan KC.** Pulmonary vascular input impedance is a combined measure of pulmonary vascular resistance and stiffness and predicts clinical outcomes better than pulmonary vascular resistance alone in pediatric patients with pulmonary hypertension. *Am Heart J* 155: 166–174, 2008.
19. **León-Velarde F, Villafuerte FC, Richalet JP.** Chronic mountain sickness and the heart. *Prog Cardiovasc Dis* 52: 540–9, 2010.
20. **Levin M, Pincott JR, Hjelm M, Taylor F, Kay J, Hoizel H, Dinwiddie R, Matthew DJ.** Hemorrhagic shock and encephalopathy: clinical, pathologic, and biochemical features. *J Pediatr* 114: 194–203, 1989.
21. **Linde T, Sandhagen B, Hägg A.** Blood viscosity and peripheral vascular resistance in patients with untreated essential hypertension. *J Hypertens* 11: 731–736, 1993.
22. **Mahapatra S, Nishimura a R, Oh JK, McGoon MD.** The prognostic value of pulmonary vascular capacitance determined by Doppler echocardiography in patients with pulmonary arterial hypertension. *J Am Soc Echocardiogr* 19: 1045–1050, 2006.
23. **Milnor WR, Nichols WW.** A new method of measuring propagation coefficients and characteristic impedance in blood vessels. *Circ Res* 36: 631–639, 1975.
24. **Milnor WR.** *Hemodynamics*. Baltimore, MD: Williams & Wilkins, 1982.
25. **Mitchell G, Pfeffer M, Westerhof N, Pfeffer J.** Measurement of aortic input impedance in rats. *Am J Physiol Heart Circ Physiol* 267: H1907–H1915, 1994.
26. **Morpurgo M, Jezek V, Ostadal B.** Pulmonary input impedance or pulmonary vascular resistance? *Monaldi Arch Chest Dis* 50: 282–285, 1995.
27. **Moudgil R, Michelakis ED, Archer SL.** Hypoxic pulmonary vasoconstriction. *J Appl Physiol* 98: 390–403, 2005.
28. **Porterfield JE, Kottam A, Raghavan K, Escobedo D, Jenkins JT, Larson ER, Treviño RJ, Valvano JW, Pearce a J, Feldman MD.** Dynamic correction for parallel conductance, GP, and gain factor, alpha, in invasive murine left ventricular volume measurements. *J Appl Physiol* 107: 1693–1703, 2009.
29. **Pratali L, Allemann Y, Rimoldi SF, Faita F, Hutter D, Rexhaj E, Brenner R, Bailey DM, Sartori C, Salmon CS, Villena M, Scherrer U, Picano E, Sicari R.** RV contractility and exercise-induced pulmonary hypertension in chronic mountain sickness: a stress echocardiographic and tissue Doppler imaging study. *JACC Cardiovasc Imaging* 6: 1287–1297, 2013.
30. **Späni D, Arras M, König B, Rülicke T.** Higher heart rate of laboratory mice housed individually vs. in pairs. *Lab Anim* 37: 54–62, 2003.

31. **Stergiopulos N, Meister J, Westerhof N.** Evaluation of methods for estimation of total arterial compliance. *Am J Physiol Heart Circ Physiol* 268: H1540–H1548, 1995.
32. **Stone H, Thompson H, Schmidt-Nielsen K.** Influence of erythrocytes on blood viscosity. *Am J Physiol* 214: 913–918, 1968.
33. **Tabima DM, Hacker TA, Chesler NC.** Measuring right ventricular function in the normal and hypertensive mouse hearts using admittance-derived pressure-volume loops. *Am J Physiol Heart Circ Physiol* 299: H2069–H2075, 2010.
34. **Tabima DM, Roldan-Alzate A, Wang Z, Hacker a T, Molthen RC, Chesler NC.** Persistent vascular collagen accumulation alters hemodynamic recovery from chronic hypoxia. *J Biomech* 45: 799–804, 2012.
35. **Tian L, Chesler NC.** In vivo and in vitro measurements of pulmonary arterial stiffness: a brief review. *Pulm Circ* 2: 505–517, 2012.
36. **Vanderpool RR, Chesler NC.** Characterization of the isolated, ventilated, and instrumented mouse lung perfused with pulsatile flow. *J. Vis. Exp.*: 3–7, 2011.
37. **Vanderpool RR, Kim AR, Molthen R, Chesler NC.** Effects of acute Rho kinase inhibition on chronic hypoxia-induced changes in proximal and distal pulmonary arterial structure and function. *J Appl Physiol* 110: 188–198, 2011.
38. **Vanderpool RR, Naeije R, Chesler NC.** Impedance in isolated mouse lungs for the determination of site of action of vasoactive agents and disease. *Ann Biomed Eng* 38: 1854–1861, 2010.
39. **Wang SH, Lee LP, Lee JS.** A linear relation between the compressibility and density of blood. *J Acoust Soc Am* 109: 390, 2001.
40. **Wang Z, Chesler NC.** Pulmonary vascular wall stiffness: An important contributor to the increased ventricular afterload with pulmonary hypertension. *Pulm Circ* 1: 212–223, 2011.
41. **Weed R, LaCelle P, Merrill E.** Metabolic dependence of red cell deformability. *J Clin Invest* 48: 795–809, 1969.
42. **Westerhof N, Sipkema P, Van Den Bos G, Elzinga G.** Forward and backward waves in the arterial system. *Cardiovasc Res* 6: 648–656, 1972.
43. **Van den Wijngaard J, Westerhof BE, Faber DJ, Ramsay MM, Westerhof N, van Gemert M.** Abnormal arterial flows by a distributed model of the fetal circulation. *Am J Physiol Regul Integr Comp Physiol* 291: R1222–R1233, 2006.
44. **Winslow RM, Monge CC, Brown EG, Klein HG, Sarnquist F, Winslow NJ, McKneally SS.** Effects of hemodilution on O_2 transport in high-altitude polycythemia. *J Appl Physiol* 59: 1495–1502, 1985.
45. **Womersley J.** The mathematical analysis of the arterial circulation in a state of oscillatory motion. *Wright Air Development Center Technical Report WADC-TR-56–614*. Dayton, OH, Wright Air Development Center, 1957.
46. **Youmans JB.** Mineral deficiencies. *J Am Med Assoc* 143: 1252–1259, 1950.
47. **Zhou Y, Zhou T, Ouzhuluobu Qiao L, Wang X, Xu H, Liu H, Hua Y.** Effect of polycythemia on hypoxia induced pulmonary hypertension and pulmonary vascular remodeling in rats. *Sichuan Da Xue Xue Bao Yi Xue Ban* 40: 619–622, 2009.